

SHADOW CORRECTIONS TO PION-DEUTERON AND PROTON-DEUTERON COLLISIONS

V. V. ANISOVICH, P. E. VOLKOVITSKIĬ and L. G. DAKHNO

Institute of High-energy Physics

Submitted May 24, 1972

Zh. Eksp. Teor. Fiz. 63, 1576—1585 (November, 1972)

High-energy shadow corrections are expressed in terms of the cross sections of inclusive processes. It is shown that shadow corrections determined with a high degree of accuracy yield additional information about the mechanism of inelastic processes. Comparison of the computed corrections with experimental values shows that antishadow effects play a significant role in rescattering for large masses in the intermediate state.

IN experiments on the scattering of π mesons by deuterons and nucleons carried out recently on the Serpukhov accelerator, the Glauber corrections^[1] to the total π -d scattering cross sections were measured with a high degree of accuracy at energy intervals of 15–60 GeV^[2]. Thus, there arose the possibility of a detailed comparison with experiment of the theoretical computations of the Glauber correction carried out under various assumptions about the mechanism of rescattering of an incident particle by the nucleons constituting the deuteron. As was indicated by Abers et al.^[3], at impinging-particle energies of the order of several GeV, besides elastic rescattering of the impinging particle by the deuteron nucleons (Fig. 1a), processes involving inelastic rescattering begin to play an appreciable role (Fig. 1b): at relativistic energies the formation of a particle group with an invariant mass M becomes possible at small momentum transfers t , so that after the interaction with the impinging particle, the nucleons agglomerate again to form a deuteron.

Let $\delta T(E, 0)$ be the shadow or Glauber correction to the scattering amplitude for a particle with energy E which undergoes zero-angle scattering on a deuteron:

$$\delta T(E, 0) = T_p(E, 0) + T_n(E, 0) - T_d(E, 0).$$

It is described by the sum of graphs of the type shown in Fig. 1 a) and b)^[4], and can be expressed in terms of the amplitude $A(t, s, s', M^2)$ of the process shown in Fig. 1c and the deuteron form factor $S(t)$:

$$\delta T(E, 0) = -\frac{1}{16\pi^2} \int_{-\infty}^{\infty} dM^2 \int_0^{\infty} dk^2 A(t, s, s'; M^2) S(4t), \quad (1)$$

where $t = -(M^2 - \mu^2)^2 / 4E^2 - k^2$, μ is the mass of the impinging particle, and $h = 2mE$ (m is the nucleon mass). The contour integration over M^2 is shown in Fig. 2.

The poles in the M^2 complex plane correspond to elastic processes in the forward and crossed M^2 channels of amplitude $A(t, s, s', M^2)$ (Fig. 1a); their contribution to the amplitude (1) and to the total cross section

$$\sigma(E) = (16\pi^2)^{-1} \text{Im } T(E, 0)$$

is called the elastic Glauber correction $\delta\sigma_{el}$. The cuts along the real axis are connected with the singularities of the amplitude $A(t, s, s', M^2)$ in the forward and crossed M^2 channels; their contribution to the integral (1) is the inelastic shadow contribution $\delta\sigma_{inel}$. The cuts in the M^2 complex plane is connected with the singularities of the form factor $S(4t)$.

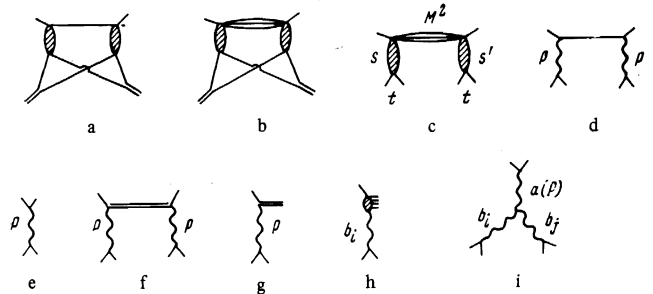


FIG. 1

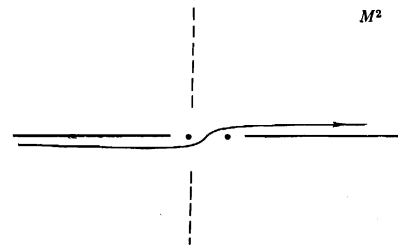


FIG. 2. The contour integration in (1).

In the inelastic-rescattering amplitude the interaction with each nucleon is realized by means of a Pomeronchuk pole exchange in the t -channel (Fig. 1d). The amplitude of each interaction with a nucleon is then almost purely imaginary. It is easy to obtain from formula (1) the usual expression^[4] for the elastic Glauber correction to the total cross section:

$$\delta\sigma_{el} = 2 \int_0^{\infty} dt \frac{d\sigma(E, t)}{dt} S(4t). \quad (2)$$

Here, $d\sigma(E, t)/dt$ is the differential cross section of elastic scattering on a nucleon (Fig. 1b); we used in the derivation of (2)

$$\text{Im } A(t, s, s, M^2) = -(16\pi^2)^{-1} \delta(M^2 - \mu^2) \frac{d\sigma(E, t)}{dt}.$$

Let us now proceed to consider the contribution of the inelastic processes to the shadow correction. At comparatively small M^2 —in the region of resonance production—the inelastic processes are similar to the elastic ones: they are due to a Pomeronchuk-pole exchange in the t -channel. In this region of M^2 the amplitude $A(t, s, s', M^2)$ can also be represented in the form of a successive exchange of P-poles (Fig. 1f). Just as in the case of the elastic rescattering, the imaginary part of

$A(t, s, s, M^2)$ is connected in this case only with the singularities in the M^2 -channel:

$$\text{Im} A(t, s, s, M^2) = -(16\pi^2)^2 \frac{d\sigma(t, E, M^2)}{dt dM^2} \text{ for } M_{\min}^2 \leq M^2 \leq M_0^2,$$

where $d\sigma(t, E, M^2)/dt dM^2$ is the cross section of inelastic production on a nucleon (Fig. 1g). For negative values of M^2 , the amplitude $A(t, s, s, M^2)$ has similar imaginary parts connected with the singularities in the crossed channel. Thus, the processes with comparatively small M^2 (diffraction dissociation) make to the shadow correction a contribution similar to that made by the elastic rescattering^[4,5]:

$$\delta\sigma_{inel}^d = 2 \int_{M_{\min}^2}^{M_0^2} dM^2 \int_{t_{\min}}^{\infty} dt \frac{d\sigma(t, E, M^2)}{dt dM^2} S(4t), \quad (3)$$

where M_0 is a quantity of the order of 2 GeV.

In the integral (1), however, $M^2 \sim E/R$ are substantial (R is the radius of the deuteron). This means that as the energy increases the range of the integration over M^2 broadens. If we represent the amplitude of the inelastic process at large M^2 in the form of a series of terms with exchange of different reggeons (one of such terms is shown in Fig. 1h; b_i is the trajectory of a reggeon), then the spectra of $d\sigma(t, E, M^2)/dt dM^2$ are described by the three-reggeon diagrams of Fig. 1i. Scale invariance of the spectra requires that $a(0)$ be equal to unity in this description, i.e., that the upper reggeon be a P-pole. The cross section $d\sigma(t, E, M^2)/dt dM^2$ can be represented in the form of a series:

$$\frac{d\sigma(t, E, M^2)}{dt dM^2} = \sum_{i,j} \frac{d\sigma(b_i^+, b_j^+)}{dt dM^2} + \sum_{i,j} \frac{d\sigma(b_i^-, b_j^-)}{dt dM^2}. \quad (4)$$

Each of the terms in this series corresponds to a contribution made by diagrams of the type shown in Fig. 1i with a positive (+) and a negative (-) signature. The individual terms in this series depend on M^2 and s as $s^{-1}(s/M^2)^{b_i + b_j - 1}$. The summation is over all possible values of i and j , and this leads to the appearance in (4) of two interference terms corresponding to the interchange of i and j .

Analysis of the three-reggeon diagrams carried out in the Appendix shows that the contribution made by large M^2 to the shadow correction can be written in the form

$$\delta\sigma_{inel}^d = \delta\sigma_{inel}^d - 2 \int_{M_0^2}^{\infty} dM^2 \int_{t_{\min}}^{\infty} dt S(4t) \times \sum_{i,j} \left\{ \frac{1}{\cos \pi b_j^+} \frac{d\sigma(b_i^+, b_j^+)}{dt dM^2} - \frac{1}{\cos \pi b_j^-} \frac{d\sigma(b_i^-, b_j^-)}{dt dM^2} \right\}. \quad (5)$$

Entering into formula (5) are terms making positive, as well as negative contributions to the Glauber correction. The negative contributions constitute an antishadow correction.

If the spectra are determined by the sum of the contributions with $b_i^+ = b_j^+ = 1$ and $b_i^- = b_j^- = 0$, then formula (5) becomes entirely similar to formula (3):

$$\delta\sigma_{inel}^{GPR} = \delta\sigma_{inel}^d + 2 \int_{M_0^2}^{\infty} dM^2 \int_{t_{\min}}^{\infty} dt S(4t) \frac{d\sigma(t, E, M^2)}{dt dM^2}. \quad (6)$$

Such a form of the shadow correction was proposed by Gribov^[4], Pumplin and Ross^[5]. If there are no antishadow terms in (5), then the Gribov-Pumplin-Ross formula yields the minimum possible—in this case—

shadow correction. Indeed, in this case, all the terms in (5) are positive, and the minimum value appears when $\cos \pi b_i^+ = -1$.

The experimental values of the spectra at fixed t (Fig. 3) outside the region of resonances practically do not depend on M^2 . Such behavior served as a basis for the description of the particle-production processes by means of diagrams with exchange in the t -channel of the poles with $b_i = \frac{1}{2}(P', \rho, \omega)$ ^[9]. As can be seen from formula (5), the description of the spectra by means of the single pole with $b_i = \frac{1}{2}$ is unsatisfactory: the amplitude $A(t, s, s, M^2)$ then becomes infinite and makes an enormous contribution to the shadow correction. Therefore, to explain the constancy of the spectra, we need some other, more complex mechanisms.

1. The constancy of the spectra can be obtained by a superposition of two or more poles with b_i close to $\frac{1}{2}$. Suppose there exist two noninterfering poles: $b_1 = \frac{1}{2} + \delta$ and $b_2 = \frac{1}{2} - \delta$. Such a mechanism provides constant spectra at large M^2 and a bounded correction to the amplitude $A(t, s, s, M^2)$. In this case

$$\delta\sigma_{inel}^{\delta} = \delta\sigma_{inel}^d - 2 \int_{M_0^2}^{\infty} dM^2 \left(1 + \frac{2}{\pi} \ln \frac{M^2}{s}\right) \int_{t_{\min}}^{\infty} dt \frac{d\sigma(t, E, M^2)}{dt dM^2} S(4t). \quad (7)$$

2. There exist two poles with $b = \frac{1}{2}$ but with different signatures. As in the previous case, the infinite parts in the amplitude $A(t, s, s, M^2)$ cancel out, and the contribution to the inelastic shadow correction from the region of large masses is finite for constant—with respect to M^2 —spectra. In this case the contribution made by large masses to the amplitude $A(t, s, s, M^2)$ is the inverse of the contribution from small masses:

$$\delta\sigma_{inel}^{+-} = \delta\sigma_{inel}^d - 2 \int_{M_0^2}^{\infty} dM^2 \int_{t_{\min}}^{\infty} dt \frac{d\sigma(t, E, M^2)}{dt dM^2} S(4t). \quad (8)$$

3. The constancy of the spectra is explained by the superposition of the diagrams with $b^+ = 1$ and $b^- = 0$. In this case the contribution of the pole with $b = 1$, which falls off as $1/M^2$, will combine with the second pole's contribution, which grows proportionally to M^2 and is an antishadow correction. We emphasize, however, that the

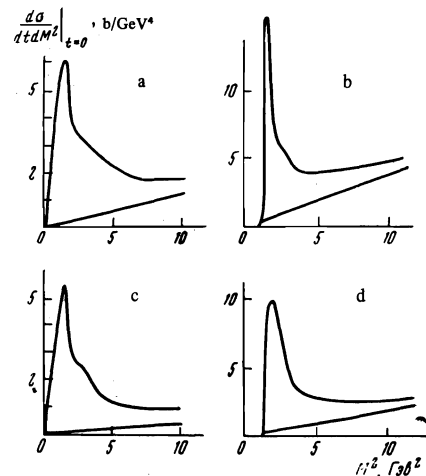


FIG. 3. Experimental spectra: a— π - p interaction, $E = 25$ GeV—according to [6]; b— π - p interaction, $E = 40$ GeV—according to [6]; c— p - p interaction, $E = 19.2$ GeV—according to [7]; d— p - p interaction, $E = 30$ GeV—according to [8].

$b = 0$ pole cannot be only a π -meson pole; for in that case, owing to the fact that an exchange of the state with isospin 1 occurs in the t -channel, the neutron yield should, in the corresponding range of values of momentum, be two times higher than the proton yield. This is at variance with experiment. The formula for the inelastic shadow correction (with allowance for inelastic charge exchange) has the form

$$\delta\sigma_{inel}^{10} = \delta\sigma_{inel}^d + 2 \int_{M_0^2}^{\infty} dM^2 \int_{t_{min}}^{\infty} dt S(4t) \left\{ \frac{d\sigma(b=1)}{dt dM^2} - \frac{d\sigma(b=0)}{dt dM^2} \right\}. \quad (9)$$

The results of numerical computations carried out with the formulas (6)–(9) are shown in Table I. The spectra shown in Fig. 3 were used in the computations; the deuteron form factor was determined from experimental data^[10] and was chosen in the form

$$S(t) = 0.55e^{a_1 t} + 0.45e^{a_2 t},$$

$$a_1 = 19.66 \text{ GeV}^{-2}, \quad a_2 = 4.67 \text{ GeV}^{-2}.$$

In Fig. 4 are shown the results of the computations, together with the experimental values of the Glauber corrections in π -d^[2] and p-d^[11-13] collisions. The errors in the computed shadow corrections are connected mainly with the errors in the experimental determination of the index of the exponential function in the dependence of the spectra on t (Table II). Furthermore, the considerable error in the computations with the formulas (7) and (8) leads to an inaccurate determination of the value of M_0 at which a change of regime occurs in the behavior of the spectra. The values cited correspond to $M_0 = 2 \text{ GeV}$.

Comparison of the experimental data with the results of the computations shows that antishadow effects of the inelastic processes with large M^2 make an appreciable contribution to the Glauber correction. Indeed, as has already been mentioned, the minimum, purely shadow contribution from large M^2 is determined by the Gribov-Pumplin-Ross formula, i.e., formula (6). The experimental values for the shadow corrections lie substan-

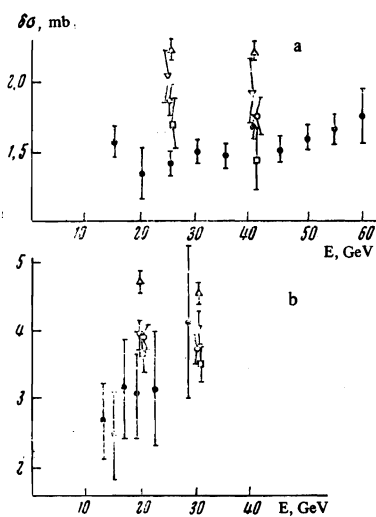


FIG. 4. Shadow corrections $\delta\sigma = \delta\sigma_{el} + \delta\sigma_{inel}$ for a- π -d interactions, and b-p-d interactions: Δ represents $\delta\sigma_{inel}$ computed from formula (6), ∇ - $\delta\sigma_{inel}^d$ computed from formula (7), \square - $\delta\sigma_{inel}^+$ computed from formula (8), and \circ - $\delta\sigma_{inel}^{10}$ computed from formula (9); the dots (\bullet) represent experimental data for a) π -d collisions^[2] and b) p-d collision^[11-13].

Table I

E, GeV	$\delta\sigma_{el}$, mb	$\delta\sigma_{inel}^{GPR}$, mb	$\delta\sigma_{inel}^{10}$, mb	$\delta\sigma_{inel}^{+-}$, mb	$\delta\sigma_{inel}^d$, mb
p-d interactions					
19.2	3.37±0.06	1.33±0.15	0.55±0.20	0.39±0.25	0.71±0.25
30	3.30±0.06	1.28±0.18	0.44±0.22	0.25±0.26	0.72±0.26
π -d interactions					
25	1.34±0.03	0.89±0.08	0.53±0.12	0.38±0.24	0.70±0.24
40	1.30±0.03	0.92±0.09	0.44±0.13	0.17±0.23	0.63±0.23

Table II. The nucleon quantities $b(E, M^2)$ [GeV^{-2}]

p-p collisions			π -p collisions		
M^2 , GeV^2	E = 19.2 GeV	30 GeV	M^2 , GeV^2	E = 25 GeV	40 GeV
1.20–1.75	20 ± 4	17 ± 4	0.04–3	7.7 ± 0.4	7.7 ± 0.4
1.75–2.00	14 ± 3	22 ± 5	3–5	6.1 ± 0.8	5.7 ± 0.8
2.00–2.50	5 ± 0.5	6 ± 1	5–7	—	5.2 ± 0.8
>2.50	5 ± 0.5	5 ± 0.5	>7	—	5.2 ± 0.8

tially below the values given by this formula. Such a reduction in the shadow correction can be caused only by antishadow effects.

The study of shadow corrections, using deuteron as an example, may prove to be quite an effective tool for the elucidation of the structure of inclusive processes in the region of small M^2/s . This is connected with the fact that in formula (5) figures an additional factor $1/\cos \pi b$ which enhances the contribution of the reggeons with b close to $1/2$.

The authors are profoundly grateful to Yu. M. Anti-pov, L. G. Landsberg, and Yu. D. Prokoshkin for a discussion of the experimental situation, and to V. N. Gribov, A. B. Kaidalov, and L. A. Kondratyuk for theoretical discussions.

APPENDIX

Let us consider the simplest six-line diagram of the three-reggeon type shown in Fig. 5. Its amplitude is equal to

$$A_{bb}(t, s, s', M^2) = \frac{1}{s^2} \int \frac{d^4 k}{(2\pi)^4 i} \frac{A(s_1, k^2) B(s_2, t, k^2) B(s_2', t, k^2)}{(k^2 - \mu^2)^2 [(k-q)^2 - \mu^2]}. \quad (A.1)$$

We shall assume that the two-particle amplitudes A and B for large s_1 and s_2 have the Regge asymptotic form

$$A(s_1) = \frac{A}{\sin \pi a} \left\{ \left(-\frac{s_1}{m_0^2} \right)^a + \left(\frac{s_1}{m_0^2} \right)^a \right\},$$

$$B(s_2, t) = \frac{B(t)}{\sin \pi b(t)} \left\{ \left(-\frac{s_2}{m_0^2} \right)^{b(t)} + \left(\frac{s_2}{m_0^2} \right)^{b(t)} \right\},$$

where m_0^2 is some quantity (which may be a function of k^2) of the order of the particle masses. This notation is, of course, arbitrary. The addend $(-s_1/m_0^2)^a$ has, in fact, a right-hand cut starting from some finite value of s_1 —from $s_1 = m_{S_1}^2$, say. At the upper shore (the physical region) of this cut this term has the complex phase

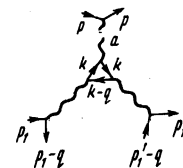


FIG. 5

$e^{-i\pi a}$, and at the lower shore, the phase $e^{i\pi a}$. Similarly, the term $(s_1/m_0^2)^a$ has a left-hand (a u-channel) cut starting from $s_1 = -m_{S_1}^2$, and the lower shore of this cut is the physical region.

Let us introduce the Sudakov variables^[14]:

$$\begin{aligned} p &= \bar{p} + \gamma \bar{p}_1, \quad p_1 = \bar{p}_1 + \gamma \bar{p}, \quad \bar{p}^2 = \bar{p}_1^2 = 0, \quad \gamma = m^2/s; \\ q &= \beta \bar{p} + \alpha \bar{p}_1 + q_\perp, \quad p_1' = \beta' \bar{p} + \alpha' \bar{p}_1 + p_{1\perp}, \quad k = \beta \bar{p} + \alpha \bar{p}_1 + k_\perp; \quad (A.2) \\ q_\perp^2 &= -q^2, \quad p_{1\perp}^2 = -p_1'^2, \quad k_\perp^2 = -k^2. \end{aligned}$$

We consider the amplitude in the region where $(p + q)^2 = M^2 \ll s = (p + p_1)^2$ and $s' = (p + p_1')^2 \sim s$. Then

$$\alpha_q \approx \frac{M^2}{s}, \quad \beta_q \approx \frac{t}{s} - \frac{m^2 M^2}{s^2}, \quad t = -q^2, \quad \alpha' = \frac{s'}{s}, \quad \beta' = \frac{t - 2M^2}{M^2}.$$

Leaving in the arguments of the integrand only the dominant terms in the expansion in powers of s and M^2 , we obtain

$$\begin{aligned} A_{bb}(t, s, s', M^2) &= \frac{1}{2s} \frac{1}{(2\pi)^4} \int d\alpha d\beta d^2k \\ &\times \frac{A(-s\alpha)B(\beta s, q^2)B(\beta s', q^2)}{(\alpha\beta s - k^2 - \mu^2)^2[(\alpha - \alpha_q)\beta s - (k - q)^2 - \mu^2]}. \quad (A.3) \end{aligned}$$

The product ABB consists of eight terms. These terms will be denoted by $A(s_1, s_2, s_2')$, $A(u_1, s_2, s_2')$, etc., depending on whether the s - or the u -channel part is chosen in the amplitudes A and B . Let us consider the term $A(s_1, s_2, s_2')$ (we set, for simplicity, $q = 0$):

$$\begin{aligned} A(s_1, s_2, s_2') &= \frac{1}{2s} \frac{1}{(2\pi)^4} AB^2 \int \frac{d\alpha d\beta d^2k}{(\alpha\beta s - k^2 - \mu^2)^2[(\alpha - \alpha_q)\beta s - k^2 - \mu^2]} \\ &\times \left(-\frac{\alpha s}{m_0^2} \right)^a \left(\frac{\beta s}{m_0^2} \right)^b \left(\frac{\beta s'}{m_0^2} \right)^b. \quad (A.4) \end{aligned}$$

In the β plane the integrand has two cuts: $-\beta s = m^2(s_2)$ and $-\beta s' = m^2(s_2')$, and two poles:

$$\beta_1 = \frac{k^2 + \mu^2}{\alpha s}, \quad \beta_2 = \frac{k^2 + \mu^2}{(\alpha - \alpha_q)s}.$$

When $\alpha < 0$, all the singularities are located in the upper half-plane, and the integral over β is equal to zero. When $0 < \alpha < \alpha_q$, the pole $k^2 = \mu^2$ passes over to the lower half-plane, and when $\alpha > \alpha_q$, also the pole $(k - q)^2 = \mu^2$ (Fig. 6a) and b). Deforming the contour of integration in the β plane to include the poles, we obtain

$$\begin{aligned} A(s_1, s_2, s_2') &= \frac{-2\pi i}{2s(2\pi)^4} AB^2 \int_{\alpha_q}^{\infty} d\alpha \\ &\times \frac{1}{(\alpha - \alpha_q)s} \left[\frac{(-\alpha s/m_0^2)^a (\beta s/m_0^2)^b (\beta s'/m_0^2)^b}{(\alpha\beta s - k^2 - \mu^2)^2} \right]_{\beta=\beta_2} \\ &+ \int_0^{\alpha_q} d\alpha \frac{1}{(\alpha s)^2} \left[\frac{d}{d\beta} \frac{(-\alpha s/m_0^2)^a (\beta s/m_0^2)^b (\beta s'/m_0^2)^b}{(\alpha - \alpha_q)\beta s - k^2 - \mu^2} \right]_{\beta=\beta_1}. \quad (A.5) \end{aligned}$$

The three-reggeon amplitude should have the form $(M^2)^a (s/M^2)^b (s'/M^2)^b$, i.e., three must be a root-type singularity in α_q . The second term in (A.5) does not have such a singularity and should therefore be dropped.

Making a change of variables $\alpha = \alpha_q x$ in the first term, we obtain

$$A(s_1, s_2, s_2') = e^{-i\pi a} (M^2)^a \left(\frac{s}{M^2} \right)^b \left(\frac{s'}{M^2} \right)^b \frac{C}{s^2}. \quad (A.6)$$

If $q \neq 0$, then

$$A(s_1, s_2, s_2') = e^{-i\pi a} (M^2)^a \left(\frac{s}{M^2} \right)^{b(-q^2)} \left(\frac{s'}{M^2} \right)^{b(-q^2)} \frac{C(q^2)}{s^2}.$$

The other terms in the amplitude $A(t, s, s', M^2)$ differ from this term by only a phase. For example,

$$\begin{aligned} A(s_1, u_2, s_2') &= \frac{1}{2s} \frac{1}{(2\pi)^4} AB^2 \int \frac{d\alpha d\beta d^2k}{(\alpha\beta s - k^2 - \mu^2)^2[(\alpha - \alpha_q)\beta s - k^2 - \mu^2]} \\ &\times \left(-\frac{\alpha s}{m_0^2} \right)^a \left(-\frac{\beta s}{m_0^2} \right)^b \left(\frac{\beta s'}{m_0^2} \right)^b = e^{-i\pi b} A(s_1, s_2, s_2'). \quad (A.7) \end{aligned}$$

Thus, the entire three-reggeon amplitude can be written in the form

$$\begin{aligned} A_{bb}(t, s, s', M^2) &= \frac{(M^2)^{a-2b} + (-M^2)^{a-2b}}{\sin \pi(2b-a)} \frac{(s)^{b(t)} + (-s)^{b(t)}}{\sin \pi b} \\ &\times \frac{(s')^{b(t)} + (-s')^{b(t)}}{\sin \pi b} \frac{R(t)}{s^2} = e^{-i\pi a/2} \frac{(M^2)^a (s/M^2)^{b(t)} (s'/M^2)^{b(t)}}{\sin \pi(b-a/2) \sin^2(\pi b/2)} \frac{R(t)}{s^2}. \quad (A.8) \end{aligned}$$

Here, the coefficient R may, of course, depend in some unknown fashion on a and b . In this formula the factors $[\sin \pi(2b-a)]^{-1} [\sin \pi b]^{-2}$ have, for convenience, been separated out in explicit form. It is interesting to note, however, that in the diagram in Fig. 5 being considered here, the function R does not, after separating out these factors, vanish at $a = 2b$. A method for writing down the three-reggeon amplitude, similar to (A.8), has been discussed by A. B. Kačalov (private communication).

The phase factor of the amplitude $A(t, s, s', M^2)$ is determined only by the phase of the upper reggeon and is equal to $e^{-i\pi a/2}$ ^[15]. To obtain the cross section $d\sigma(t, E, M^2)/dt dM^2$ we must in the amplitude $A(t, s, s', M^2)$ take s' to the second sheet and then take the imaginary part (or the jump with respect to M^2). The contribution to the cross section from the three-reggeon diagram in Fig. 1h is equal to

$$\begin{aligned} \frac{d\sigma(t, E, M^2)}{dt dM^2} &= \frac{1}{(16\pi^2)^2} \sin \pi \left(b - \frac{a}{2} \right) e^{i\pi a/2} A_{bb}(t, s, s, M^2) \\ &= \frac{R(t) (M^2)^a (s/M^2)^{2b}}{(16\pi^2 s)^2 \sin^2(\pi b/2)}. \quad (A.9) \end{aligned}$$

We emphasize that this connection arose only because of the structure of the dependence of the amplitude A on M^2 , s' , and s .

If the inelastic processes are due to several Regge poles, then there appear three-reggeon diagrams in which all the reggeons are different. The structure of such diagrams is similar to the structure analyzed above. If one of the lower poles has a trajectory b and the other pole, the trajectory b' , then the amplitude of such a three-reggeon diagram is obtained from (A.8) by replacing in the first (M^2 -dependent) factor, $2b - a$, by $b + b' - a$ and in the last (s' -dependent) factor, b by b' . Two such interfering diagrams, differing by the interchange of b and b' , make the following total contribution to the differential cross section:

$$\begin{aligned} \frac{d\sigma(b, b')}{dt dM^2} + \frac{d\sigma(b', b)}{dt dM^2} &= \\ &= \frac{1}{(16\pi^2)^2} \left[\sin \pi \left(b - \frac{a}{2} \right) + \sin \pi \left(b' - \frac{a}{2} \right) \right] e^{i\pi a/2} A_{bb'}(t, s, s, M^2) = \\ &= 2 \cos \frac{\pi}{2} (b - b') \frac{R'(t) (M^2)^a (s/M^2)^{b+b'}}{(16\pi^2 s)^2 \sin(\pi b/2) \sin(\pi b'/2)}. \quad (A.10) \end{aligned}$$

If the lower reggeons have a negative signature, then

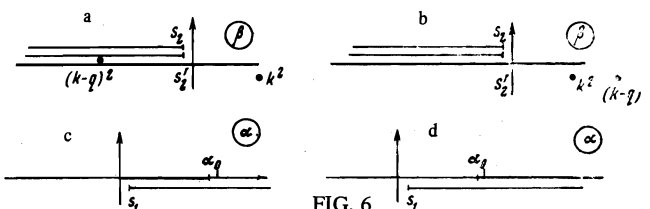


FIG. 6

$$A_{b-b^-}(t, s, s', M^2) = -e^{-ia/2} \frac{(M^2)^a (s/M^2)^{b(t)} (s'/M^2)^{b(t)} R^-(t)}{\sin \pi(b-a/2) \cos^2(\pi b/2) s^2}, \quad (\text{A.11})$$

and the cross section is connected with the amplitude $A_{b-b^-}(t, s, s, M^2)$ by the relation

$$\frac{d\sigma(b^-, b^-)}{dt dM^2} = -\frac{1}{(16\pi^2)^2} \sin \pi \left(b - \frac{a}{2} \right) e^{ia/2} A_{b-b^-}(t, s, s, M^2) = \frac{R^-(t) (M^2)^a (s/M^2)^{2b}}{(16\pi^2 s)^2 \cos^2(\pi b/2)}. \quad (\text{A.12})$$

The formulas (A.9)–(A.11) lead to formula (5).

¹R. J. Glauber, Phys. Rev. **100**, 242 (1955).

²Yu. P. Gorin, S. P. Denisov, S. V. Donskov, et al., Preprint IFVÉ, (Inst. of High Energy Physics), pp. 71–100.

³F. S. Abers, H. Burchardt, V. L. Teplitz, and C. Wilkin, Nuovo Cimento **42**, 363 (1966).

⁴V. N. Gribov, Zh. Eksp. Teor. Fiz. **56**, 892 (1968) [Sov. Phys.-JETP **29**, 483 (1969)].

⁵J. Pumplin and M. Ross, Phys. Rev. Lett. **21**, 1778 (1968).

⁶Y. M. Antipov, R. Baud, R. Busnello, et al., Papers

submitted to the 4th Int. Conf. on High-energy Collisions, Oxford, 1972.

⁷J. V. Allaby, B. Binon, A. N. Diddens, et al., Preprint CERN 70-12, 1970.

⁸E. W. Anderson, E. J. Bleser, G. B. Collins, et al., Phys. Rev. Lett. **19**, 198 (1967).

⁹C. Risk and J. H. Friedman, Phys. Rev. Lett. **27**, 353 (1971).

¹⁰J. E. Elias, J. I. Friedman, G. C. Hartmann, et al., Phys. Rev. **177**, 2075 (1969).

¹¹K. J. Foley, R. S. Jones, S. J. Lindenbaum, et al., Phys. Rev. Lett. **19**, 330, 857 (1967).

¹²L. W. Jones, M. J. Longo, T. P. McCorriston, et al., Phys. Lett. **36B**, 509 (1971).

¹³J. Engler, K. Horn, and J. König, Phys. Lett. **27B**, 599 (1969).

¹⁴V. V. Sudakov, Zh. Eksp. Teor. Fiz. **30**, 87 (1956) [Sov. Phys.-JETP **3**, 65 (1956)].

¹⁵O. V. Kancheli and S. G. Matinyan, Yad. Fiz. **11**, 1305 (1970) [Sov. J. Nucl. Phys. **11**, 726 (1970)].

Translated by A. K. Ageyi

173